33rd Annual International Conference of the IEEE EMBS
Boston, Massachusetts USA, August 30 - September 3, 2011

Development of a Novel Six-Axis Force/Moment Sensor Attached to a Prosthetic Limb for the Unrestrained Gait Measurement

Yuichiro Hayashi, Nobutaka Tsujiuchi, Takayuki Koizumi and Hiroko Oshima
Department of Mechanical Engineering, Doshisha University
1-3, Miyakodani, Tatara, Kyotanabe-City, Kyoto, 610-0321, JAPAN
etj1302@mail4.doshisha.ac.jp, ntsujiuc@mail.doshisha.ac.jp, tkoizumi@mail.doshisha.ac.jp, oshima.hiroko@gmail.com

Youtaro Tsuchiya
Tec Gihan Co., LTD
1-22, Nishinohata, Okubo-Town, Uji-City, Kyoto, 611-0033, JAPAN
y.tsuchiya@tecgihan.co.jp

***Abstract*—Since the number of trans-femoral amputees has increased by industrial or traffic accidents in modern society, a prosthetic limb has been required. In this case, those amputees must regain moving pattern by efficient gait training using load conditions on a prosthetic limb as quantitative evaluation indices. However, conventional gait training systems cannot measure long continuous walking motions. In this paper, a novel six-axis force/moment sensor, which is attached to a prosthetic limb for the unrestrained gait measurement, is developed. As a result of applying response surface method and desirability function, optimum design variables to reduce interference components are obtained. Finally, characteristics test by applying optimum design variables is performed and the effectiveness of the developed sensor is validated.**

I. Introduction

ALTHOUGH safety control and accident prevention are emphasized in modern society, number of lower limb amputees has increased by industrial or traffic accidents. Since more amputees require a prosthetic limb, its needs have increased year after year [1]. They must substitute the artificial knee joint of trans-femoral prosthesis for their lost ones. In this case, unsteady gait frequently arises from a mismatch between their kinesthetic senses and load conditions on a prosthetic limb in common activities; however, it is hard to regain moving pattern by previous methods. Therefore, load conditions need to be measured as quantitative evaluation indices for efficient gait training.

In a past study, a multi-axis force/moment sensor can measure loads applied on lower limb prosthesis has been developed as a gait training system; however, it cannot measure long continuous walking motions because there are problems that signal processing section works separately from measuring section and PC must be connected [2].

In this paper, we aim to develop a novel six-axis force/moment sensor which can be attached to a prosthetic limb for the unrestrained gait measurement. Response surface method and desirability function are used for structural optimization of this sensor to make the effect of interference components much smaller. Finally, characteristics test using the production model by applying optimum design variables and the effectiveness of this sensor is validated.

II. A Novel Six-Axis Force/Moment Sensor

A. Design of Sensor

Figure 1 shows the prototype of this sensor. This sensor can be attached to a prosthetic limb as shown in Fig. 2 and can measure loads by a total of 32 strain gauges in the elastic body. Load ratings are as follows: F_x, F_y, F_z are 1000[N], M_x, M_y are 100[N·m] and M_z is 50[N·m]. Besides, A7075 and A2024 are used as the materials. This sensor features integration of measuring section and signal processing section by embedded data logger and can measure long continuous data without PC by battery and memory card.

B. Measurement Principle

Figure 3 shows a diagram of surfaces and position coordinates with strain gauges. This sensor can calculate corresponding strains to each axial load component by compounding outputs from eight full-bridge circuits. Gauge 1, 4 are strain gauges put on the direction parallel to the neutral axis of beams and gauge 2, 3 are strain gauges put at a 45 [deg] angle to the neutral axis. Arithmetic expressions of strains are represented as below by corresponding outputs of strains $\varepsilon_{A1},...,\varepsilon_{G4}$ and $\varepsilon_{F_x}, \varepsilon_{F_y}, \varepsilon_{F_z}, \varepsilon_{M_x}, \varepsilon_{M_y}, \varepsilon_{M_z}$ with each strain gauge and each axial load component.

$$\varepsilon_{F_x} = \varepsilon_{B1} - \varepsilon_{A1} + \varepsilon_{B4} - \varepsilon_{A4} + \varepsilon_{E1} - \varepsilon_{F1} + \varepsilon_{E4} - \varepsilon_{F4} \quad (1)$$

$$\varepsilon_{F_y} = \varepsilon_{D1} - \varepsilon_{C1} + \varepsilon_{D4} - \varepsilon_{C4} + \varepsilon_{G1} - \varepsilon_{H1} + \varepsilon_{G4} - \varepsilon_{H4} \quad (2)$$

$$\varepsilon_{F_z} = \varepsilon_{A2} - \varepsilon_{A3} + \varepsilon_{B2} - \varepsilon_{B3} + \varepsilon_{E2} - \varepsilon_{E3} + \varepsilon_{F2} - \varepsilon_{F3} + \varepsilon_{C2} - \varepsilon_{C3} + \varepsilon_{D2} - \varepsilon_{D3} + \varepsilon_{G2} - \varepsilon_{G3} + \varepsilon_{H2} - \varepsilon_{H3} \quad (3)$$

$$\varepsilon_{M_x} = \varepsilon_{A2} - \varepsilon_{A3} + \varepsilon_{B2} - \varepsilon_{B3} - \varepsilon_{E2} + \varepsilon_{E3} - \varepsilon_{F2} + \varepsilon_{F3} \quad (4)$$

$$\varepsilon_{M_y} = \varepsilon_{C2} - \varepsilon_{C3} + \varepsilon_{D2} - \varepsilon_{D3} - \varepsilon_{G2} + \varepsilon_{G3} - \varepsilon_{H2} + \varepsilon_{H3} \quad (5)$$

$$\varepsilon_{M_z} = \varepsilon_{B1} - \varepsilon_{A1} + \varepsilon_{B4} - \varepsilon_{A4} + \varepsilon_{D1} - \varepsilon_{C1} + \varepsilon_{D4} - \varepsilon_{C4} - \varepsilon_{E1} + \varepsilon_{F1} - \varepsilon_{E4} + \varepsilon_{F4} - \varepsilon_{G1} + \varepsilon_{H1} - \varepsilon_{G4} + \varepsilon_{H4} \quad (6)$$

C. Evaluation Method of Force/Moment Sensor

In this paper, the quantitative evaluation method proposed by Uchiyama et al. [3] and Nakamura et al. [4] is used to evaluate performance of force/moment sensor. Relational expression between load matrix $\boldsymbol{f}$ and corresponding strain matrix $\boldsymbol{\varepsilon}$ is described below by strain compliance matrix $\boldsymbol{C}$.

$$\boldsymbol{\varepsilon} = \boldsymbol{C}\boldsymbol{f} \tag{7}$$

where

$$\boldsymbol{f}_j = (F_{xj} \quad F_{yj} \quad F_{zj} \quad M_{xj} \quad M_{yj} \quad M_{zj})^T \tag{8}$$

$$\boldsymbol{\varepsilon}_j = (\varepsilon_{F_x j} \quad \varepsilon_{F_y j} \quad \varepsilon_{F_z j} \quad \varepsilon_{M_x j} \quad \varepsilon_{M_y j} \quad \varepsilon_{M_z j})^T \tag{9}$$

$\boldsymbol{\varepsilon} = (\boldsymbol{\varepsilon}_1 \quad \cdots \quad \boldsymbol{\varepsilon}_n)$, $\boldsymbol{f} = (\boldsymbol{f}_1 \quad \cdots \quad \boldsymbol{f}_n)$, $j = 1, ..., n$, and n is a data number. If $\boldsymbol{\varepsilon}$, $\boldsymbol{f}$ are normalized by maximal values to negate units and $\bar{\boldsymbol{\varepsilon}}$, $\bar{\boldsymbol{f}}$ are derived, (7) is described below.

$$\bar{\boldsymbol{\varepsilon}} = \bar{\boldsymbol{C}}\bar{\boldsymbol{f}} \tag{10}$$

Derived strain compliance matrix $\bar{\boldsymbol{C}}$ is generated by $\bar{\boldsymbol{\varepsilon}}$, $\bar{\boldsymbol{f}}$ and made by arranging more than six applied loads and strain data respectively. $\bar{\boldsymbol{C}}$ is obtained by postmultiplying $\bar{\boldsymbol{\varepsilon}}$ by $\bar{\boldsymbol{f}}^+$ as a pseudo-inverse matrix of $\bar{\boldsymbol{f}}$. Each row vector norm, minimal singular value and $\lambda_{\max}/\lambda_{\min}$ as maximal singular value divided by minimal singular value concerning $\bar{\boldsymbol{C}}$ are defined as strain gauge sensitivity $\left\|\bar{\boldsymbol{C}}_i\right\|$, force sensitivity $\lambda_{\min}$ and condition number $\mathrm{cond}.\bar{\boldsymbol{C}}$, and these values are used for evaluation. If force/moment sensor has ideal structure, it can measure each independent load component, and sensitivities are equivalent each other. Therefore, $\bar{\boldsymbol{C}}$ becomes a unit matrix and each evaluation index becomes equal to 1.

D. Sensitivity Evaluation of the Prototype

Corresponding strains with each axial load component are obtained by finite element analysis of the prototype and sensitivity evaluation is performed by strain compliance matrix. Used finite element model is shown in Fig. 4. I-deas 11 and NX Nastran Ver. 4.1 made by UGS PLM Solutions Co., LTD are used as 3D CAD and structural analysis software. Analysis conditions are as follows: longitudinal elastic modulus and density of A7075 and A2024 are 71.0 [GPa] and 72.4 [GPa], 2.80×10^3 [kg/m^3] and 2.77×10^3 [kg/m^3], Poisson's ratio is 0.33 and each load rating is singularly applied to the top surface of the elastic body when both ends are restrained. In addition, x and y-axis directions are equivalent to the others. Equations (11)-(14) show each evaluation index by way of example in the analytical results.

$$\bar{\boldsymbol{C}} = \begin{pmatrix} 0.183 & 8.91\times10^{-4} & 2.23\times10^{-4} & -2.94\times10^{-2} & -0.504 & 3.57\times10^{-3} \\ 8.91\times10^{-4} & 0.183 & 2.23\times10^{-4} & -0.504 & -2.94\times10^{-2} & 3.57\times10^{-3} \\ 3.13\times10^{-4} & 3.13\times10^{-4} & 0.110 & -5.02\times10^{-3} & -5.02\times10^{-3} & -1.08\times10^{-2} \\ 1.19\times10^{-3} & -0.299 & -8.93\times10^{-5} & 1.02 & 5.20\times10^{-3} & -5.30\times10^{-5} \\ -0.299 & 1.19\times10^{-3} & -8.93\times10^{-5} & 5.20\times10^{-3} & 1.02 & -5.30\times10^{-5} \\ -4.09\times10^{-4} & -4.09\times10^{-4} & 2.69\times10^{-3} & -1.19\times10^{-2} & -1.19\times10^{-2} & 1.61 \end{pmatrix} \tag{11}$$

$$\left\|\bar{\boldsymbol{C}}_1\right\| = 0.537, \ \left\|\bar{\boldsymbol{C}}_2\right\| = 0.537, \ \left\|\bar{\boldsymbol{C}}_3\right\| = 0.111, \\ \left\|\bar{\boldsymbol{C}}_4\right\| = 1.06, \ \left\|\bar{\boldsymbol{C}}_5\right\| = 1.06, \ \left\|\bar{\boldsymbol{C}}_6\right\| = 1.61 \tag{12}$$

$$\lambda_{\min} = 0.0248 \tag{13}$$

$$\mathrm{cond}.\bar{\boldsymbol{C}} = 65.0 \tag{14}$$

III. Structural Optimization of This Sensor

Structural optimization of this sensor is performed by response surface method and desirability function. JMP 6 made by SAS Institute Japan Ltd. and MATLAB 2007a made by The MathWorks, Inc. are used for DOE and calculation. First, domains for design variables are determined. Five design variables shown in Fig. 5 are as follows: x_1, x_2: Position coordinates of gauge 2 and 3, gauge 1 and 4, x_3: Height from the neutral axis of beam to the top edge, x_4: Radius of internal hole, x_5: Projection length of outer edges. Domains of x_1, x_2 are defined by the area of beam as below.

$$4.80\,[\mathrm{mm}] \le x_1 \le 14.0\,[\mathrm{mm}] \tag{15}$$

$$4.80\,[\mathrm{mm}] \le x_2 \le 14.5\,[\mathrm{mm}] \tag{16}$$

Design dimensions of the prototype upper limit are defined as x_3, x_4, x_5. Height of gauge 1 h is as below.

$$h = 8.00/2 + 1.40/2 = 4.70\,[\mathrm{mm}] \tag{17}$$

Therefore, domains of x_3, x_4, x_5 are as below.

$$4.70\,[\mathrm{mm}] \le x_3 \le 6.25\,[\mathrm{mm}] \tag{18}$$

$$0\,[\mathrm{mm}] \le x_4 \le 15.1\,[\mathrm{mm}] \tag{19}$$

$$0\,[\mathrm{mm}] \le x_5 \le 2.00\,[\mathrm{mm}] \tag{20}$$

Secondly, objective functions and constraint conditions are clarified. Diagonal elements of strain matrix $\varepsilon_{F_x}(\varepsilon_{F_y})$, $\varepsilon_{F_z}, \varepsilon_{M_x}(\varepsilon_{M_y}), \varepsilon_{M_z}$ are defined as objective functions and design variables maximizing those values simultaneously are determined. Then, constraint condition is defined as below because maximal von Mises equivalent stress $\sigma_{\max}$ must be less than or equal to proof stress of A7075 σ_Y = 515 [MPa] divided by safety factor $S = 2$ under all load ratings.

$$\sigma_{\max} \le \sigma_Y / S = 257.5\,[\mathrm{MPa}] \tag{21}$$

Third, quadratic approximations of objective functions and constraint condition $\hat{\varepsilon}_{F_x}, \hat{\varepsilon}_{F_z}, \hat{\varepsilon}_{M_x}, \hat{\varepsilon}_{M_z}, \hat{\sigma}_{\max}$ by finite element analysis and response surface method are determined below.

$$\hat{\varepsilon}_{F_x} = 1.94\times10^{-4} - 2.29\times10^{-4} z_2 - 3.62\times10^{-5} z_3 \\ + 1.23\times10^{-4} z_4 + 4.42\times10^{-5} z_2 z_3 - 1.40\times10^{-4} z_2 z_4 \tag{22}$$

$$\hat{\varepsilon}_{F_z} = 1.49\times10^{-4} - 1.64\times10^{-4} z_1 + 7.34\times10^{-5} z_4 - 8.23\times10^{-5} z_1 z_4 \tag{23}$$

$$\hat{\varepsilon}_{M_x} = 6.37\times10^{-4} - 1.40\times10^{-3} z_1 - 6.95\times10^{-5} z_2 - 7.57\times10^{-5} z_3 \\ + 7.40\times10^{-4} z_4 - 8.27\times10^{-5} z_5 - 7.69\times10^{-4} z_1 z_4 + 1.27\times10^{-4} z_2 z_4 \\ - 1.37\times10^{-4} z_3 z_4 - 1.34\times10^{-4} z_2 z_5 + 1.25\times10^{-4} z_3 z_5 \\ + 2.67\times10^{-4} {z_1}^2 + 4.50\times10^{-4} {z_4}^2 + 3.30\times10^{-4} {z_5}^2 \tag{24}$$

$$\hat{\varepsilon}_{M_z} = 4.16\times10^{-4} - 1.17\times10^{-3} z_2 + 1.18\times10^{-4} z_3 \\ + 4.57\times10^{-4} z_4 + 1.14\times10^{-4} z_2 z_3 - 5.40\times10^{-4} z_2 z_4 \\ + 5.79\times10^{-4} {z_2}^2 + 2.78\times10^{-4} {z_3}^2 - 5.18\times10^{-2} {z_5}^2 \tag{25}$$

$$\hat{\sigma}_{\max} = 137 + 0.667 z_1 + 0.111 z_2 - 11.4 z_3 + 17.2 z_4 + 2.22 z_5 \\ - 10.9 z_3 z_4 + 3.37 {z_1}^2 + 3.37 {z_2}^2 + 7.37 {z_4}^2 + 3.37 {z_5}^2\,[\mathrm{MPa}] \tag{26}$$

where $z_i\ (i = 1, ..., 5)$ are levels of x_i. Relation between level z and design variable x is as below when $X_{\max}, X_{\min}$ are values of corresponding design variables to levels 1 and -1.

$$z = \frac{X_{\max} - X_{\min}}{2} x + \frac{X_{\max} + X_{\min}}{2} \tag{27}$$

Fourth, desirability function to put response surfaces in a pile is determined. It is that $d_j(Y_j) = 1$ is satisfied and $d_j(Y_j) = 0$ is not satisfied regarding objective functions $Y_j\ (j = 1, ..., m)$. Final objective function D is as follows.

$$D = \left\{ \prod_{j=1}^{m} d_j(Y_j) \right\}^{\frac{1}{m}} \tag{28}$$

Optimization problem is solved by obtaining a solution when (28) is maximized. Function form has various types; however, it is defined as follows because Y_j must be maximized.

$$d_j(Y_j)=\begin{cases}0 & Y_j<L_j\\ \left(\dfrac{Y_j(x_1,\ldots,x_5)-L_j}{T_j-L_j}\right)^s & L_j\le Y_j<T_j\\ 1 & Y_j\ge T_j\end{cases} \tag{29}$$

where T_j is target value, L_j is lower limit and s is arbitrary constant. $T_j=1.00\times10^{-3}, L_j=-1.00\times10^{-3}$ when $j=1,2$ and $T_j=1.00\times10^{-2}$, $L_j=-1.00\times10^{-2}, s=1$ when $j=3,4$. For these reasons, D is described below.

$$\begin{aligned}D&=\left\{d(\hat{\varepsilon}_{F_x})d(\hat{\varepsilon}_{F_z})d(\hat{\varepsilon}_{M_x})d(\hat{\varepsilon}_{M_z})\right\}^{\frac{1}{4}}\\ &=\left\{\begin{matrix}6.25\times10^8(\hat{\varepsilon}_{F_x}+1.00\times10^{-3})(\hat{\varepsilon}_{F_z}+1.00\times10^{-3})\\ \times(\hat{\varepsilon}_{M_x}+1.00\times10^{-2})(\hat{\varepsilon}_{M_z}+1.00\times10^{-2})\end{matrix}\right\}^{\frac{1}{4}}\end{aligned} \tag{30}$$

Fifth, sequential quadratic programming as mathematical programming is used to solve this problem. As a result of the calculation with constraint condition as below, optimum solution is obtained as each design variable $x_1=4.80[\mathrm{mm}]$, $x_2=4.80[\mathrm{mm}], x_3=4.70[\mathrm{mm}], x_4=15.1[\mathrm{mm}], x_5=2.00[\mathrm{mm}]$.

$$\text{minimize}\quad f(z)=-\left\{\begin{matrix}6.25\times10^8(\hat{\varepsilon}_{F_x}+1.00\times10^{-3})(\hat{\varepsilon}_{F_z}+1.00\times10^{-3})\\ \times(\hat{\varepsilon}_{M_x}+1.00\times10^{-2})(\hat{\varepsilon}_{M_z}+1.00\times10^{-2})\end{matrix}\right\}^{\frac{1}{4}} \tag{31}$$

$$z=(z_1,\ldots,z_5)^T\in\boldsymbol{R}^5$$

$$\text{subject to}\quad \hat{\sigma}_{\max}\le257.5, -1\le z_i\le1\,(i=1,\ldots,5) \tag{32}$$

IV. Performance Evaluation of This Sensor

A. Sensitivity Evaluation of the Optimized Sensor

Sensitivity evaluation is performed again to validate the effectiveness of this sensor by applying optimum design variables. Analysis condition is the same as chapter 2 basically. Each obtained evaluation index is as follows by way of example in the analytical results.

$$\overline{\boldsymbol{C}}=\begin{pmatrix}0.199 & -5.35\times10^{-3} & 4.72\times10^{-5} & 9.09\times10^{-3} & -6.95\times10^{-2} & 1.03\times10^{-4}\\ -5.35\times10^{-3} & 0.199 & 4.72\times10^{-5} & -6.95\times10^{-2} & 9.09\times10^{-3} & 1.03\times10^{-4}\\ -1.84\times10^{-3} & -1.84\times10^{-3} & 0.126 & 6.41\times10^{-2} & 6.41\times10^{-2} & -1.37\times10^{-2}\\ 5.11\times10^{-2} & -0.335 & -1.67\times10^{-3} & 1.13 & 1.80\times10^{-2} & -1.55\times10^{-2}\\ -0.335 & 5.11\times10^{-2} & -1.67\times10^{-3} & 1.80\times10^{-2} & 1.13 & -1.55\times10^{-2}\\ 7.78\times10^{-3} & 7.78\times10^{-3} & -3.15\times10^{-3} & -2.58\times10^{-2} & -2.58\times10^{-2} & 1.82\end{pmatrix} \tag{33}$$

$$\left\|\overline{\boldsymbol{C}}_1\right\|=0.211,\ \left\|\overline{\boldsymbol{C}}_2\right\|=0.211,\ \left\|\overline{\boldsymbol{C}}_3\right\|=0.155,$$
$$\left\|\overline{\boldsymbol{C}}_4\right\|=1.18,\ \left\|\overline{\boldsymbol{C}}_5\right\|=1.18,\ \left\|\overline{\boldsymbol{C}}_6\right\|=1.82 \tag{34}$$

$$\lambda_{\min}=0.124 \tag{35}$$

$$\mathrm{cond}.\overline{\boldsymbol{C}}=14.8 \tag{36}$$

B. Characteristics Test

Characteristics test is performed by fabricated production model applying optimum design variables to validate the effectiveness of this sensor. For F_x, F_y and M_x, M_y, each load is applied to this sensor to 490.0[N] per 98.0[N], to 29.5[N·m] per 5.9[N·m], respectively when this sensor and weight of 10 [kg] are attached to the tester with wire as shown in Fig. 6 and Fig. 7. For M_z, load is applied to this sensor to 24.5[N·m] per 4.9[N·m] when this sensor and weight of 2 [kg] are attached to the tester with wire and pulley as shown in Fig. 8. For F_z, load is applied to this sensor to 1000[N] per 200[N] when it is attached to the tester as shown in Fig. 9.

Obtained experimental results are shown in Figs. 10-13. As a result of sensitivity evaluation concerning experimental results, each evaluation index is obtained as below.

$$\overline{\boldsymbol{C}}=\begin{pmatrix}0.192 & 2.09\times10^{-2} & 1.49\times10^{-3} & -5.17\times10^{-2} & 8.56\times10^{-2} & 8.66\times10^{-3}\\ -1.74\times10^{-3} & 0.198 & 2.13\times10^{-3} & -9.06\times10^{-2} & -2.11\times10^{-2} & 1.23\times10^{-2}\\ 1.32\times10^{-2} & -5.48\times10^{-3} & 0.122 & 4.73\times10^{-3} & 1.77\times10^{-2} & -2.46\times10^{-3}\\ 7.89\times10^{-3} & -0.444 & -2.09\times10^{-3} & 1.11 & 9.50\times10^{-3} & 1.85\times10^{-2}\\ 0.443 & 1.75\times10^{-3} & -2.12\times10^{-3} & -5.64\times10^{-3} & 1.14 & 1.47\times10^{-2}\\ 1.84\times10^{-2} & -2.54\times10^{-2} & 3.81\times10^{-3} & 2.26\times10^{-2} & 1.80\times10^{-2} & 1.84\end{pmatrix} \tag{37}$$

$$\left\|\overline{\boldsymbol{C}}_1\right\|=0.217,\ \left\|\overline{\boldsymbol{C}}_2\right\|=0.219,\ \left\|\overline{\boldsymbol{C}}_3\right\|=0.124,$$
$$\left\|\overline{\boldsymbol{C}}_4\right\|=1.20,\ \left\|\overline{\boldsymbol{C}}_5\right\|=1.22,\ \left\|\overline{\boldsymbol{C}}_6\right\|=1.84 \tag{38}$$

$$\lambda_{\min}=0.121 \tag{39}$$

$$\mathrm{cond}.\overline{\boldsymbol{C}}=15.2 \tag{40}$$

C. Consideration

Intercomparison between (11)-(14) and (33)-(36) shows increased diagonal elements and decreased corresponding off-diagonal elements of F_x, F_y to M_x, M_y in $\overline{\boldsymbol{C}}$ of the optimized sensor. Therefore, it is assumed that force sensitivity and condition number are greatly improved by diagonalized $\overline{\boldsymbol{C}}$. In addition, characteristics test is compared with finite element analysis concerning sensitivity evaluation results and it is found that each value is nearly equivalent to the others by (33)-(36) and (37)-(40). For these reasons, this sensor can measure each axial load component independently and the effectiveness of the developed sensor is validated.

V. Conclusion

In this paper, a novel six-axis force/moment sensor which can be attached to a prosthetic limb for the unrestrained gait measurement has developed. Response surface method and desirability function are used for structural optimization and it reduces interference components. Finally, as a result of performance evaluation using finite element analysis and characteristics test by applying optimum design variables, it can measure self-decoupled each axial load component and the effectiveness of the developed sensor is validated.

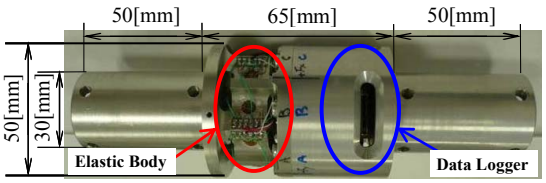

Fig. 1. Prototype of a six-axis force/moment sensor.

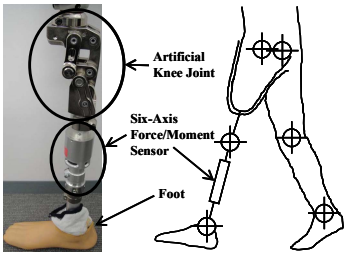

Fig. 2. Attachment position of a six-axis force/moment sensor.

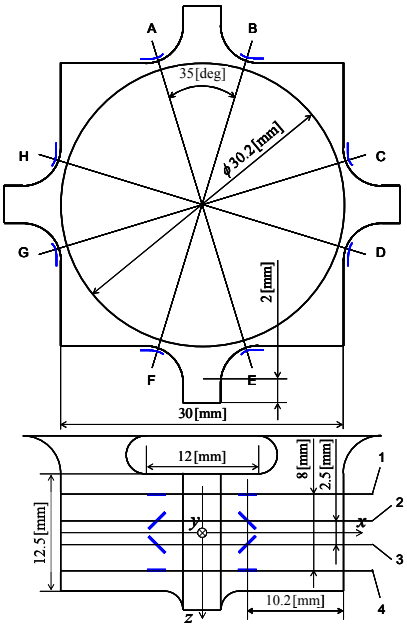

Fig. 3. Placing surface and coordinates of strain gauges.

Fig. 4. Finite element model of the prototype.

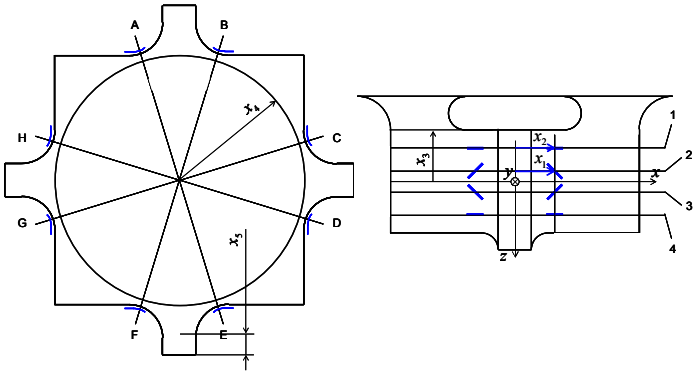

Fig. 5. Design variables.

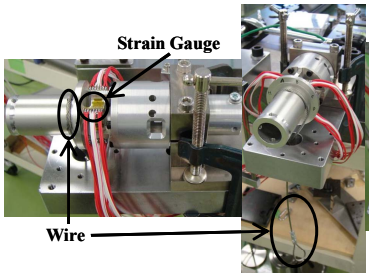

(a) Lateral view (b) Front view

Fig. 6. Load means of F_x, F_y.

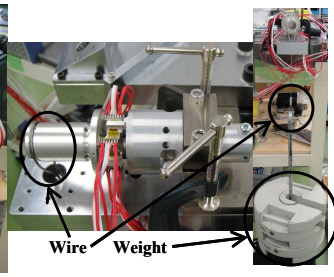

(a) Lateral view (b) Suspended weight

Fig. 7. Load means of M_x, M_y.

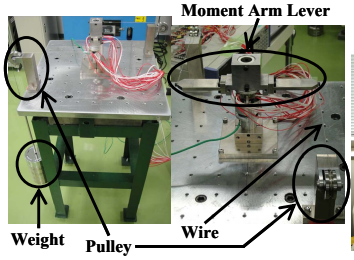

(a) Testing stand (b) Torsion by wire

Fig. 8. Load means of M_z.

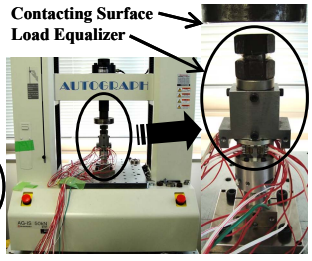

(a) Front view (b) Pressed sensor

Fig. 9. Load means of F_z.

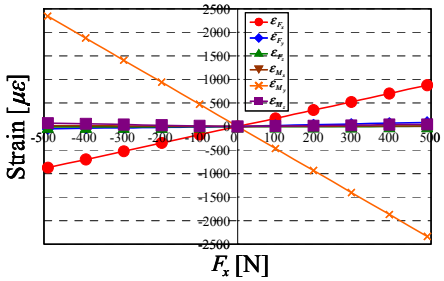

Fig. 10. Each output of strain to F_x.

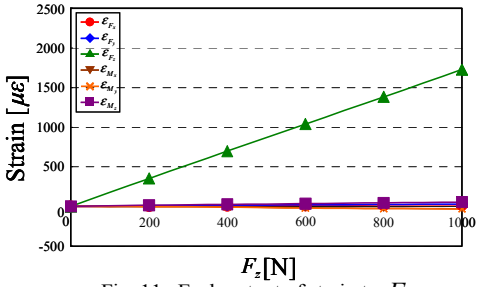

Fig. 11. Each output of strain to F_z.

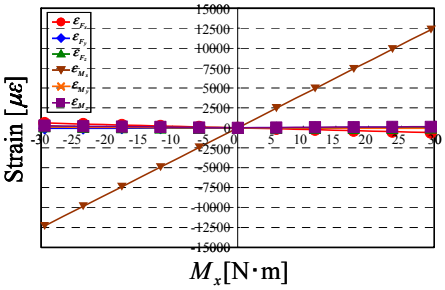

Fig. 12. Each output of strain to M_x.

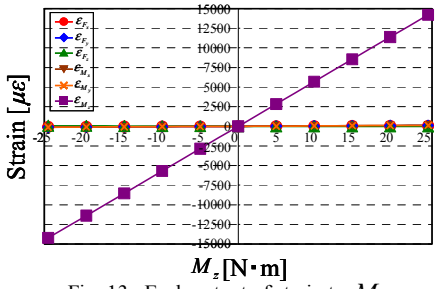

Fig. 13. Each output of strain to M_z.

ACKNOWLEDGMENT

This study was partially supported by Grant-in-Aid for Scientific Research (A)(23246041), Japan Society for the Promotion of Science.

REFERENCES

[1] S. Sawamura, *Amputation and prosthetic limb*. vol. 4, Ishiyaku Publication, 2004, pp. 1–5.

[2] A. Nakagawa, H. Matsubara, Y. Nagakura and S. Morimoto, "Development of a prosthetic gait training system for geriatric amputees," Report Collection in Hyogo Prefectural Welfare Engineering Laboratory, 2003, pp. 181–186.

[3] M. Uchiyama, K. Hakomori and Y. Nakamura, "Structural evaluation of robotic force/moment sensor by singular value decomposition," *Journal of Robotics Society of Japan*, vol. 5, no. 1, pp. 4–10, 1987.

[4] Y. Nakamura, T. Yoshikawa and I. Futamata, "Elastic component design criteria and signal processing of force sensors," *Journal of Society of Instrument and Control Engineers*, vol. 23, no. 5, pp. 433–439, 1987.